

## Micro-SAXS and force/strain measurements during the tensile deformation of single struts of an elastomeric polyurethane foam

C. Martin,<sup>a</sup> G. Eeckhaut,<sup>b</sup> A. Mahendrasingam,<sup>a</sup> D. J. Blundell,<sup>a,c</sup> W. Fuller,<sup>a\*</sup> R. J. Oldman,<sup>c</sup> S. J. Bingham,<sup>a</sup> T. Dieing<sup>d</sup> and C. Riekell<sup>d</sup>

<sup>a</sup>Department of Physics, Keele University, Keele, Staffordshire ST5 5BG, UK, <sup>b</sup>Polymer Science Group, R&D Department, Huntsman Polyurethanes (formerly ICI Polyurethanes), Everslaan 45, B-3078 Kortenberg, Belgium, <sup>c</sup>ICI R&T Centre, PO Box 90, Wilton Centre, Middlesbrough, Cleveland TS90 8JE, UK, and <sup>d</sup>ESRF, BP 220, F-38043 Grenoble CEDEX, France. E-mail: pha40@keele.ac.uk

(Received 3 November 1999; accepted 12 April 2000)

A microdeformation stage based on a piezoelectric crystal actuator capable of measuring the force applied to micrometre-sized polymeric samples is described. Laboratory force/strain measurements on a single strut of an elastomeric polyurethane foam have been conducted for the first time. The device has also been used on the microfocus beamline at the European Synchrotron Radiation Facility to collect microbeam small-angle X-ray scattering data simultaneously with strain and force measurements during the time-resolved tensile deformation of a single strut of elastomeric polyurethane foam.

**Keywords:** micro-SAXS; microdeformation; polyurethane foam; stress/strain measurement.

### 1. Introduction

The use of X-ray synchrotron radiation for the study of structural variation in synthetic polymers is a well established technique. *In situ* experiments of polymer phase transformations were pioneered by Zachmann *et al.* (Elsner *et al.*, 1985) and this remains a very active field. Recent examples are in the study of structural development processes such as melt crystallization (Terrill *et al.*, 1998; Hsiao *et al.*, 1995), strain-induced crystallization (Mahendrasingam *et al.*, 1999; Blundell *et al.*, 1995) and reactive processing (Elwell *et al.*, 1997; Ryan *et al.*, 1991). Often the development of specialized techniques and sample environments has been necessary, for both wide-angle X-ray scattering (WAXS) (Pople *et al.*, 1997), small-angle X-ray scattering (SAXS) (Bras & Ryan, 1998) and simultaneous SAXS/WAXS (Creagh *et al.*, 1998; Hughes *et al.*, 1996; Ryan *et al.*, 1994).

For WAXS experiments the high brilliance of third-generation synchrotron radiation sources, such as the European Synchrotron Radiation Source (ESRF), has allowed the size of the X-ray beam at the sample to be reduced to micrometre and submicrometre levels. WAXS studies of polymeric systems now routinely use collimation systems (Dreher *et al.*, 1995; Mahendrasingam *et al.*, 1995) and capillary optics (Riekell *et al.*, 1997; Martin *et al.*, 1997) to produce beams of these dimensions. It has recently been shown that SAXS techniques can be employed in experiments with beams of a few micrometres in size, although

the resolution was limited to about 15 nm (Riekell *et al.*, 1998; Waigh *et al.*, 1998). In the present paper we will show that by slightly relaxing the beam diameter to 10  $\mu\text{m}$  it is now possible to perform micro-SAXS experiments with the same resolution and flux as was achievable 15 years ago with a beam of millimetre dimensions at second-generation synchrotron radiation sources (Elsner *et al.*, 1985). These techniques have been extended to include the possibility of on-line time-resolved WAXS or SAXS during deformation of single polymeric fibres by the design of a microdeformation stage based on a piezoelectrically driven actuator. Micro-WAXS experiments from single ultrahigh-molecular-weight polyethylene fibres (UHMW-PE) have already been conducted using a prototype device (Riekell *et al.*, 1999). In this article we describe instrumentation capable of combining micro-SAXS with force and strain measurements from single struts of an elastomeric polyurethane (PU) foam on the microfocus beamline (ID13) at the ESRF.

### 2. Experimental techniques

For cellular foams the structure observed from a bulk sample of the material is a combination of contributions from many randomly oriented and dispersed structural units (the 'struts') and junctions (the 'plateau regions') of the cellular structure (Gibson & Ashby, 1997). The small physical size of a single strut of a PU foam presents such

severe handling difficulties that for convenience it has commonly been assumed that the properties of the strut can be adequately represented by those of the foam in bulk. Typically, foam struts are of the order of tens of micrometres in section and a few hundreds of micrometres in length. Fig. 1 is a scanning-electron-microscope (SEM) image of an elastomeric PU foam, with a single strut highlighted. With the new instrumentation it is now possible to address the uncertainty in earlier assumptions by the application of microdeformation techniques where force and strain measurements have been combined with the micro-SAXS capability of beamline ID13 in the study of polymer samples with dimensions of tens of micrometres.

The microdeformation stage used in this study was a development of the prototype used for WAXS experiments on UHMW-PE fibres (Riekkel *et al.*, 1999) and was based on a commercially available piezo-driven optical slit device from Piezosystem Jena. The device base was  $42 \times 42 \times 7$  mm and had a solid-state flexure hinged parallelogram design, which allowed a symmetrical displacement about the centre line. Special sample-mounting jaws were constructed to replace the slit mounts and the whole assembly was mounted on a crystallographic goniometer. A significant advantage of using a piezoelectric actuator was that, although the total travel was limited to about 230  $\mu\text{m}$ , the controls required were relatively simple and it was possible to control the displacement of the sample-mounting jaws with precision. In addition, the comparatively high force produced by the piezoelectric actuator meant that the contribution of the resistance of the sample to the total compliance of the device was negligible.

Typically, the samples had a gauge length in the range 100–150  $\mu\text{m}$  (this being set by manually adjusting the zero-volt gap between the sample-mounting jaws), an approxi-

mately triangular cross section and an area in the range from about  $1 \times 10^{-9} \text{ m}^2$  to  $1 \times 10^{-8} \text{ m}^2$ . Depending on the sample size, a maximum strain of between 1.5 and 2.5 was achievable at maximum actuator extension under these conditions. A precision miniature force transducer of type ELJ manufactured by Entran Limited and capable of being mounted on one of the sample-mounting jaws was specified and two interchangeable units were used with ranges 0.2 N and 0.5 N. One end of the sample was attached to the transducer measuring beam and the other end was attached to the second jaw.

The handling and mounting of samples as small as those described above is a significant difficulty and Huntsman Polyurethanes (formerly ICI Polyurethanes) have developed microhandling equipment and techniques which allow a single strut of foam to be separated from the bulk and mounted on the microdeformation stage. Care was taken during this procedure to minimize any stress applied to the struts as any pre-experiment strain could influence the integrity of the measurements. Physically attaching such small and delicate samples to the mounting jaws was also problematic and, in the case of the experiments described in this study, the struts were attached directly using an epoxy-resin-based adhesive. The tension applied to the piezoelectric actuator was varied *via* a variable potential divider fitted across the output from a high-tension laboratory power supply. By this method it was possible to calibrate the sample jaw displacement and device hysteresis as a function of applied voltage in the laboratory. A more sophisticated control would be possible using a closed-loop feedback system which sensed the jaw displacement to give a positional resolution and stability in the nanometre range, but this was not utilized in this application. Fig. 2 shows a schematic drawing of the deformation stage with a sample attached.

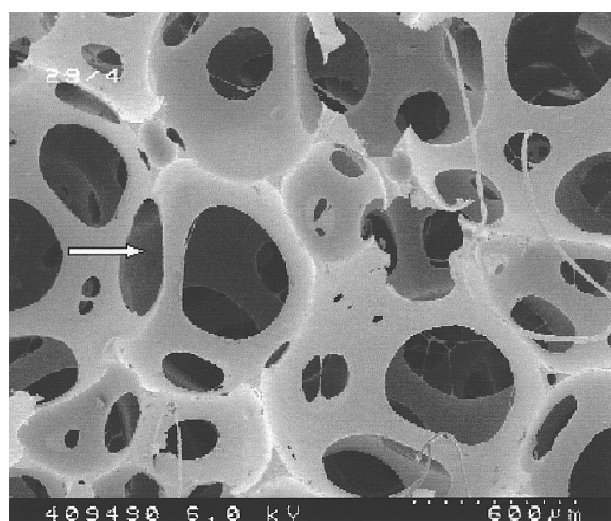


**Figure 1**

An SEM image of the structure of a foam of the type used in this work. The arrow indicates a single strut of approximate dimensions 80  $\mu\text{m}$  in section and 300  $\mu\text{m}$  in length, which was typical of the ones investigated.

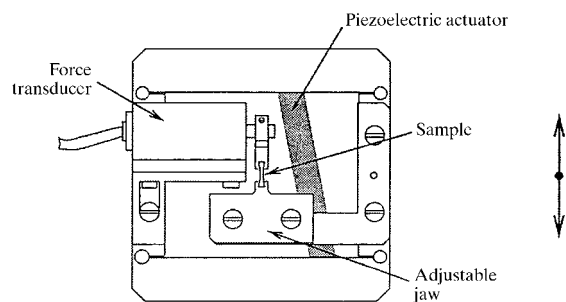


**Figure 2**

Simplified diagram of the microdeformation stage. The static zero-volt gap between the sample-mounting jaws was adjusted manually before mounting the sample. Typically the gap would be set at between 100 and 150  $\mu\text{m}$ . The extension of the piezoelectric actuator distorted the parallelogram structure of the device *via* elastic deformation of the solid-state flexure hinges. The arrows on the right-hand side represent the movement of the jaws relative to the X-ray beam: the movement of the sample-mounting jaws was symmetrical about the centre line. The sizes of the sample and of the gap have been exaggerated for clarity.

The microdeformation stage was then mounted onto a standard crystallographic goniometer head which in turn was attached to the Physik Instrumente precision *X/Y* stage on ID13. The sample was initially aligned with a reference point in an off-line high-resolution optical microscope and was then translated into the X-ray beam by the movement of a three-axis motorized gantry. The coordinates of the optical reference point and the X-ray beam position were calibrated by a WAXS experiment with a reference sample. Positional accuracy of  $<5\ \mu\text{m}$  was thus obtained.

The force applied to the sample was measured directly from the digital display of the excitation/amplifier module which had been previously calibrated to the specific force transducer. In the case of both applied voltage and force, measurements could be taken either visually from digital displays or captured by a PC data-acquisition system. The strain applied to the sample was deduced for each voltage setting from the calibration curves generated in the laboratory. Static SAXS patterns and force data were collected as the strain of the sample was incrementally increased and decreased. Suitable 'blank' exposures were collected to allow the subtraction of background scattering during subsequent data analysis.

The optical configuration used for the experiments was based on microcollimation using a  $10\ \mu\text{m}$ -diameter collimator with a  $20\ \mu\text{m}$ -diameter post-collimator guard aperture, which provided a  $7\ \mu\text{m}$  FWHM beam. The flux density in this configuration had been determined as  $\leq 2 \times 10^7\ \text{photons s}^{-1}\ \mu\text{m}^{-2}\ \text{mA}^{-1}$  at  $15.8\ \text{keV}$  (Riekel *et al.*, 1998). With an evacuated SAXS tube in this configuration it was possible to cleanly resolve the third-order reflection of dry rat's tail collagen ( $216.6\ \text{\AA}$ ). A Photonic Science CCD detector and Synoptics framegrabber were used as the X-ray data-collection system (Hughes *et al.*, 1996). It has more recently been shown that, with careful alignment and the use of a higher-resolution CCD (MAR) detector, the first order of dry rat's tail collagen can be resolved using this configuration. A schematic diagram of the experimental set-up is shown in Fig. 3.

### 3. Results and discussion

The struts used in this investigation were selected from a block of a typical flexible PU foam based on an aromatic isocyanate with a 'hard' block volume fraction of  $\sim 0.25$  with a molecular weight between crosslinks of  $\sim 4000\ \text{Da}$ . Initially, a series of nominal stress/strain measurements were conducted off-line in the laboratory associated with ID13 and the results presented here represent, for the first time, an indication of the stress/strain behaviour of single struts of a foamed polymer. Subsequently, with the beam-line optics optimized for micro-SAXS and able to resolve  $\sim 250\ \text{\AA}$ , real-time measurements were made during the deformation of a single strut of PU foam, also for the first time.

#### 3.1. Force/strain measurements

In the tensile experiments the microdeformation stage was mounted under a stereomicroscope and the voltage applied to the piezoelectric transducer was incremented in steps of  $10\ \text{V}$  at  $30\ \text{s}$  intervals from zero up to the maximum of  $150\ \text{V}$ . Then the voltage was reduced back to zero in a similar manner. The separation of the jaws and the tensile force were measured at each stage in order to obtain the strain and nominal stress, respectively. A typical force *versus* strain plot is illustrated in Fig. 4. The example shows significant hysteresis and a large permanent deformation. It was not possible to determine an elasticity modulus for the struts as the first measured point was beyond the anticipated elastic region of the material. However, an estimated value for the elastic modulus is  $\sim 50\ \text{MPa}$ , based on models of PU elastomers in the bulk (Stanford, 1998).

In the stress relaxation experiment the maximum strain was imposed by quickly ramping up the voltage on the actuator from zero to  $150\ \text{V}$  over a period of  $\sim 10\ \text{s}$ . The relaxation of the tensile force was noted every  $30\ \text{s}$ . After a few minutes the voltage was switched back to zero and the relaxation of the compressive force was similarly noted.

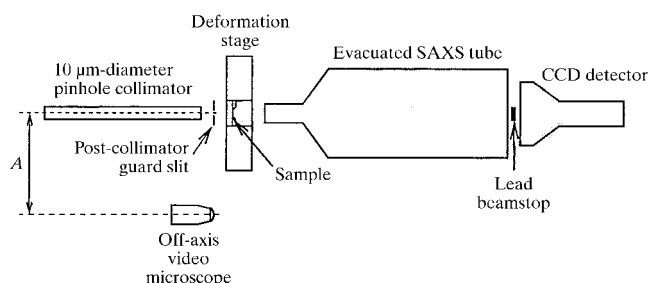


**Figure 3**

Schematic diagram of the experimental set-up. The deformation stage could be accurately translated between the microscope and X-ray beam positions. The translation distance  $A$  was pre-determined by a calibration experiment.

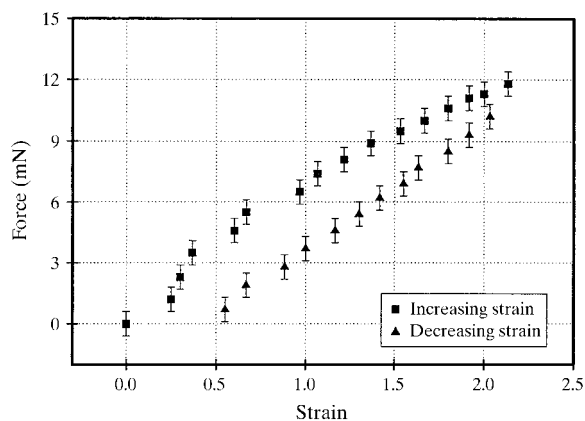


**Figure 4**

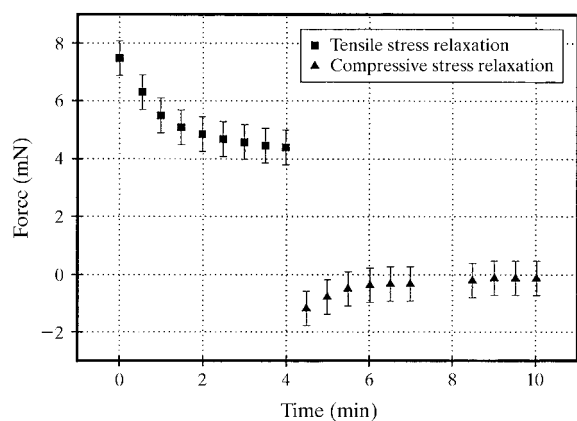
Force *versus* strain plot for a single strut of elastomeric polyurethane foam.

Fig. 5 shows a plot of the single strut relaxation data. An exponentially decaying curve fitted to the tensile data suggests a characteristic decay time of  $\sim 1$  min to a stress level about one half of the initial value. The decay in compressive stress in the second part of the experiment indicates a decay time of similar magnitude.

### 3.2. Micro-SAXS measurements

The configuration and optimization of the beamline for the collection of two-dimensional SAXS patterns from such small and weakly diffracting samples as those described was non-trivial and was in itself a major target of the investigation. Methodologies were devised to reliably position the microdeformation stage in the X-ray beam. The applicability of this approach is demonstrated in Fig. 6, which shows a SAXS pattern from a single strut mounted on the microdeformation stage before the application of any strain. It is immediately apparent that the pattern shows discrete elliptical diffraction maxima with a very marked intensification in the meridional direction. Measurements of the peak maxima indicate a  $d$  spacing of  $\sim 157$  Å along the strut axis and of  $\sim 119$  Å transverse to the strut axis. While from the two-dimensional SAXS data in Fig. 6 there is a clear indication that the mesophase morphology in the struts from this particular foam is anisotropic (and was confirmed by measurements on other samples from the same foam), we do not propose this condition as being a general one for all foams. Indeed, this is evident from the isotropic SAXS patterns obtained in parallel experiments on struts from foam samples with different chemistry where there is no evidence of an oriented morphology.

In the case of PU foams, previously only the macro-mechanical behaviour has been readily monitored (Gibson & Ashby, 1997; Hilyard, 1982; Hilyard & Cunningham, 1994). Thus there is little knowledge of the bulk properties of the polymer material from which the foam is formed. Earlier information from SAXS only related to the global average structure and cannot say whether there is structural anisotropy in individual struts within the foam. The



**Figure 5** Tensile and compressive stress relaxation plot for a single strut of elastomeric polyurethane foam.

origin of the orientation of the polymer which has been suggested by the results from this study is not clear, but could be the result of shear induced by the expansion of the foam mix during the foaming process. Such low stresses as are produced during foaming can in principle influence a microphase separating system enabling an oriented mesophase to form. There is the possibility that an anisotropic mesophase structure could change the yield properties of the polymer material.

Static micro-SAXS studies were complemented with a dynamic experiment where the sample was elongated, with strain, force and SAXS data being collected simultaneously. The methodology is illustrated by data from an experiment where a single strut of PU foam of the type illustrated in Fig. 1 was strained by increasing the voltage applied to the piezo actuator in 25 V increments from zero through to 150 V. This was equivalent to a maximum strain of  $\sim 2.1$ . Subsequently, the strain was reduced in an equivalent manner back to zero applied volts. During the collection of this data set it became apparent that the SAXS pattern was lost at strains above  $\sim 1.5$ . This could be interpreted as being due to a slight off-axis movement of the sample at higher strains, temporarily moving the sample relative to the X-ray beam. However, this loss in diffraction was not an effect in either the increasing or decreasing regimes at low strains, and at strains below  $\sim 1.5$  it has been possible to adequately analyse the data set.

The features which are discernible from those parts of the data set where SAXS patterns are evident are that, as anticipated, with increasing strain there was a reduction in the scattered intensity (probably due to sample thinning) and that, in addition, there was an increase in the measured  $d$  spacing of the diffraction maxima in the meridional

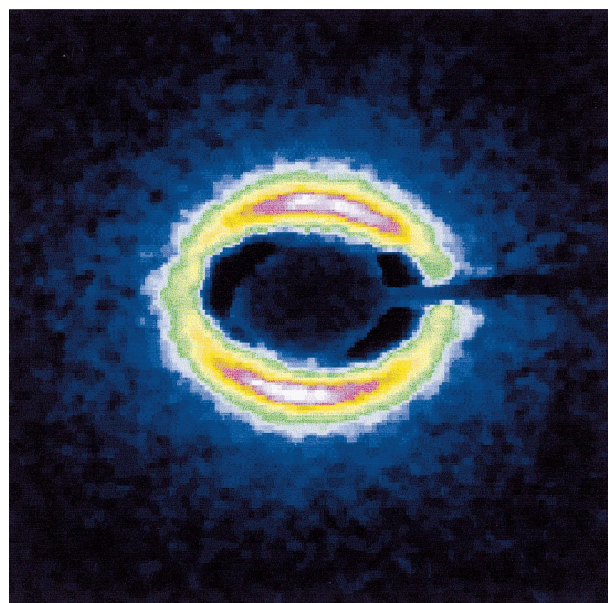


**Figure 6** Two-dimensional SAXS pattern of a single strut of elastomeric polyurethane foam before the application of strain. The strut was positioned with its axis in a vertical orientation.

direction. The variation of the  $d$  spacing of this diffraction peak as a function of strain is plotted in Fig. 7. The measured variation of  $d$  spacing can be interpreted as an increased separation of the diffracting structural units, the 'hard' blocks, permitted by the lower stiffness of the tightly coiled molecular chains in the 'soft' blocks. This phenomenon has been noted by authors in studies of tensile deformation of PUs in bulk form (Rule & Nye, 1995; Desper *et al.*, 1985). The increase in spacing may also be responsible for some reduction in the scattered intensity in the SAXS reflections as the increase in  $d$  spacing implies a tendency to move behind the backstop at higher strains.

Although there is no direct evidence in the data collected in the present experiments, it is possible to speculate another explanation for the reduction and subsequent loss in scattered SAXS intensity which was observed. Recent time-resolved simultaneous SAXS/WAXS work by Creagh *et al.* (1997) on bulk thermoplastic PU elastomers of relatively high crystallinity has shown that virtually all long- and short-range structural order can be lost in PU systems at strains above  $\sim 1.5$ . This change was reversible and was attributed to the unravelling of molecules from the 'hard' blocks and it may be that this phenomenon is paralleled in the experiments described here. Future experiments will be designed to address these uncertainties.

#### 4. Conclusions

The development of a micromanipulation technique capable of isolating and handling single struts from PU foams could be instrumental in linking bulk polymer properties to foam properties, especially in the case of water-blown polyurethane foams where the chemical generation of carbon dioxide prevents the preparation of large bulk polymer samples with the same chemical composition and morphology. The equipment described in this paper was specially developed to overcome these difficulties and to open the possibility of making structural and stress/strain measurements on small polymer samples. The force/strain measurements reported here are, to our knowledge, the first ones to be made on a single strut of a polyurethane foam. They clearly show the hysteresis and stress relaxation properties which are demonstrated by PU materials in bulk and thus provide confidence in the equipment and techniques.

Interpretation of the mechanical properties of foam is usually based on the assumption that the struts are structurally isotropic. Although limited in scope, results from the microbeam SAXS techniques described have shown that this hypothesis may not be as general as has previously been accepted. Further, the observation of anisotropy in the SAXS patterns was not predicted and, if confirmed by results from experiments where the limitations of the present techniques have been addressed, could have a fundamental significance on the development and interpretation of models of polymeric foams and their behaviour. However, it is stressed that the anisotropy observed

was not a feature of the SAXS from every sample examined. The collection, for the first time, of micro-SAXS data relied on the parallel development on ID13 at the ESRF of a suitable micrometre-sized high-brilliance X-ray beam and appropriate experimental methodologies.

The time-resolved micro-SAXS/deformation experiments demonstrated a lengthening of the  $d$  spacing associated with scattering from the 'hard' block components, but it was not possible to determine whether the reduction in scattered SAXS intensity at higher strains was due to movement of the sample within the beam or to a loss of order in the polymer structure.

We plan to further develop the equipment described in this paper to address the limitations which have been highlighted and to allow more sophisticated experiments to be conducted. In particular, it will be important to have the facility of being able to monitor on-line, and in real-time, the visual aspect of the sample. This will not only give a direct indication of the strain which has been applied to the sample, but will also provide confidence that the sample does not move relative to the X-ray beam. It will be useful to optimize the beamline optics on ID13 to increase the resolving power for micro-SAXS in order to be able to follow the changes in the SAXS pattern as a function of strain more thoroughly than has been possible so far, especially for the sample which appears to show anisotropy. We also intend to conduct experiments on a greater range of samples than the very limited number which we have investigated so far. Additionally, we intend to improve the sample-mounting technique. In the longer term the design of a cyclical stress capability for the deformation stage is planned together with the possibility of varying the sample environment.

This work was supported by grants from Huntsman Polyurethanes (formerly ICI Polyurethanes) and the

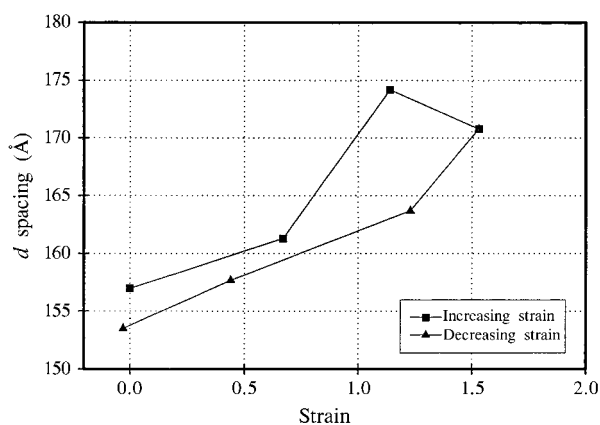


**Figure 7**

Plot of  $d$  spacing *versus* strain for an experiment where a single strut of PU foam was incrementally strained to  $\sim 2.1$ . There was a loss in diffracted SAXS intensity above a strain of  $\sim 1.5$  which is attributed either to the sample moving relative to the X-ray beam or to a loss of long-range structural order.

EPSRC (GR/M39909), and by an allocation of beam time on the microfocuss beamline ID13 at the ESRF. The microdeformation stage was built and commissioned in the Keele Physics Department. We are indebted to one of the reviewers of this paper for helpful and constructive comments which have aided the interpretations made. We are grateful to E. J. T. Greasley, M. G. Davies, M. P. Wallace and C. M. Sutton at Keele for technical and secretarial support and to L. Lardiere at the ESRF for technical support on the beamline. Acknowledgement is made to A. P. Hammersley and to the ESRF for the use of the *FIT2D* software in the analysis and presentation of the two-dimensional data in this article.

## References

- Blundell, D. J., MacKerron, D. H., Fuller, W., Mahendrasingam, A., Martin, C., Oldman, R. J., Rule, R. J. & Riekkel, C. (1995). *Polymer*, **37**, 3303–3311.
- Bras, W. & Ryan, A. J. (1998). *Adv. Colloid Interface Sci.* **75**, 1–43.
- Creagh, D. C., O'Neill, P. M. & Martin, D. J. (1997). *J. Synchrotron Rad.* **4**, 163–168.
- Creagh, D. C., O'Neill, P. M., Mills, R. J. & Holt, S. A. (1998). *J. Synchrotron Rad.* **5**, 958–961.
- Desper, C. R., Schneider, N. S. & Jasinski, J. P. (1985). *Macromolecules*, **18**, 2755–2761.
- Dreher, S., Zachmann, H. G., Riekkel, C. & Engström, P. (1995). *Macromolecules*, **28**, 7071–7074.
- Elsner, G., Riekkel, C. & Zachmann, H. G. (1985). *Advances in Polymer Science*, Vol. 67, pp. 1–57. New York: Plenum Press.
- Elwell, M. J., Ryan, A. J., Grunbauer, H. J. M. & vanLieshout, H. C. (1997). *ACS Symp. Ser.* **669**, 143–164.
- Gibson, L. J. & Ashby, M. F. (1997). *Cellular Solids: Structure and Properties*, 2nd ed., pp. 56–57. Cambridge University Press.
- Hilyard, N. C. (1982). *Mechanics of Cellular Plastics*, ch. 1. London: Applied Science Publishers.
- Hilyard, N. C. & Cunningham, A. (1994). *Low Density Cellular Plastics: Physical Behaviour*. London: Chapman and Hall.
- Hsiao, B. S., Sauer, B. B., Verma, R. K., Zachmann, H. G., Seifert, S., Chu, B. & Harney, P. (1995). *Macromolecules*, **28**, 6931–6936.
- Hughes, D. J., Mahendrasingam, A., Heeley, E. L., Oatway, W. B., Martin, C., Towns-Andrews, E. & Fuller, W. (1996). *J. Synchrotron Rad.* **3**, 84–90.
- Mahendrasingam, A., Martin, C., Fuller, W., Blundell, D. J., MacKerron, D. H., Rule, R. J., Oldman, R. J., Liggat, J., Riekkel, C. & Engström, P. (1995). *J. Synchrotron Rad.* **2**, 308–311.
- Mahendrasingam, A., Martin, C., Fuller, W., Blundell, D. J., Oldman, R. J., Harvie, J. L., MacKerron, D. H., Riekkel, C. & Engström, P. (1999). *Polymer*, **40**, 5553–5565.
- Martin, C., Mahendrasingam, A., Fuller, W., Harvie, J. L., Blundell, D. J., Whitehead, J., Oldman, R. J., Riekkel, C. & Engström, P. (1997). *J. Synchrotron Rad.* **4**, 223–227.
- Pople, J. A., Keates, P. A. & Mitchell, G. R. (1997). *J. Synchrotron Rad.* **4**, 267–278.
- Riekkel, C., Cedola, A., Heidelberg, F. & Wagner, K. (1997). *Macromolecules*, **30**, 1033–1037.
- Riekkel, C., Engström, P. & Martin, C. (1998). *J. Macromol. Sci. Phys.* **B37**, 587–599.
- Riekkel, C., Engström, P. & Vincze, L. (1999). *Étude Microstructurale des Polymères in Imagerie des Polymères*, edited by C. G'Sell. Nancy: Apollor.
- Rule, R. J. & Nye, T. M. W. (1995). *Nucl. Instrum. Methods Phys. Res. B*, **97**, 248–252.
- Ryan, A. J., Naylor, S., Komanshek, B. U., Bras, W., Mant, G. R. & Derbyshire, G. E. (1994). *ACS Symp. Ser.* **581**, 162–180.
- Ryan, A. J., Willkomm, W. R., Bergstrom, T. B., Macosko, C. W., Koberstein, J. T., Yu, C. C. & Russell, T. P. (1991). *Macromolecules*, **24**, 2883–2889.
- Stanford, J. L. (1998). In *Polymer Networks*, edited by R. T. F. Stepto, ch. 5. London: Wiley.
- Terrill, N. J., Fairclough, J. P. A., Towns-Andrews, E., Komanshek, B. U., Young, R. J. & Ryan, A. J. (1998). *Polymer*, **39**, 2381–2385.
- Waigh, T. A., Perry, P., Riekkel, C., Gidley, M. J. & Donald, A. M. (1998). *Macromolecules*, **31**, 7980–7984.